

Numerical Analysis on Static and Dynamic Behavior of Additively Manufactured BCC Lattice Structures

Muhamad Syafwan Azmi[†], Rainah Ismail^{†,‡,*}, Muhammad Nasruddin Nurdin[†], Azma Putra^{†,‡}

[†] Faculty of Mechanical Engineering, Universiti Teknikal Malaysia Melaka, Hang Tuah Jaya, 76100 Durian Tunggal, Melaka, Malaysia.

[‡] Centre for Advanced Research on Energy, Universiti Teknikal Malaysia Melaka, Hang Tuah Jaya, 76100 Durian Tunggal, Melaka, Malaysia.

*Corresponding author email: rainah@utem.edu.my

ABSTRACT

This research aims to investigate the effect of the strut diameter of lattice structures on their vibration characteristic numerically. The finite element analysis (FEA) method was validated beforehand in experimental work with lattice structure fabricated using fused deposition modeling (FDM) additive manufacturing (AM). From the comparison, good agreement was achieved with less than 11% error. From numerical results, it was found the stiffness values decrease with strut diameter from 1.8 mm to 1.0 mm. The first three vibration modes show steady increment around 12 Hz, 20 Hz, and 70 Hz in natural frequency respectively for acrylonitrile butadiene styrene (ABS) material and roughly 35 Hz, 60 Hz, and 200 Hz for both stainless steel and titanium as the strut diameter increase by 0.2 mm each. The validated FEA models can be used for exploration on many other materials and design parameters without having to conduct experimental work which helps for sustainability.

KEYWORDS

Lattice structure, Finite element analysis, Modal analysis, Vibration characteristic

INTRODUCTION

At present, with a rising requirement for energy conservation and environmental protection, researchers have put forth great efforts to pursue high energy efficiency in the design and development of engines and motors in automobiles [1]. Besides, the recent international movement of rules and regulations on fuel efficiency and passenger vehicle gas emissions have contributed to this great concern regarding vehicle weight reduction [1]. Since then, newly developed vehicles are developed with better fuel-saving technology. This can be combined with the use of lighter weight but superior mechanical performance materials such as glass and carbon fiber reinforced polymer for improved energy efficiency [2-6]. It is commonly recommended to use these materials, since not only the gross weight can be lowered, but these materials' mechanical performance can sometimes be as high or superior as that of regular metallic materials. [2,7-9]. However, substitutes for these materials need to be proposed as currently, these materials are expensive and this will eventually increase the price of vehicles. Hence, the use of cellular structure material can be suggested.

The lattice structure is one of many cellular materials that can offer a good balance of strength, stiffness, expense, resilience, promising prospects for energy absorption, and comparative static and dynamic characteristics [10-11]. Lattice structures were initiated from the approximation approach of the foam structure cellular material [12]. Lattice structures offer added advantages as compared to the anisotropic downside of the honeycomb structure where the strength of honeycomb structures is drastically reduced when the force exerted is in-plane to the honeycomb structures [13]. Also, the lattice structure is periodic and offers consistency in performance throughout the structure unlike that of the foam structure which suffers un-uniformity that compromises the overall performance due to its manufacturing technique [14]. Before the start of additive manufacturing technology, limited topological designs of lattice structures can be used. Besides that, the produced lattice structures often huge in size when using conventional manufacturing methods. Emerging technology such as additive manufacturing has gained much attention to researchers as the use of additive manufacturing allows greater

flexibility of design as opposed to the conventional method [15]. Besides that, using a conventional method such as mold/die and subtractive manufacturing using cutting tools will also contribute to waste [16]. Therefore, with AM technology, the unit cell size design parameter of lattice structures can now be rendered into a wider range from large to micro-scale lattice structures with less material used [12,17].

Present uses of cellular material lattice structures are however restricted to trivial unimportant components, particularly in dynamic applications [18]. This 'precautionary exploitation' is because the dynamic experiments linked to the performance of lattice structures cellular material have been relatively scarce, especially those made using additive manufacturing techniques. If the lattice structure is to be used because of its highly advantageous lightweight properties in dynamic applications such as body parts for moving machines and devices, dynamic testing is important to determine the suitability of this structure in such applications. Syam et al., [19] recently studied the dynamic behavior of the lattice structure made through laser powder bed fusion (LPBF). Their research comprises an experimental and numerical investigation for a vibration control isolator application. Three models were tested in the experimental study and then compared to numerical study where percentage error ranges from 0.8% to 26%. Through the validated simulation, they extended their study to a total of six models, this way, minimal experimental were conducted and hence conserve on material consumption which is good for sustainability.

Lou et al, [18] studied the effect of damage existent in lattice sandwich structure on its vibration characteristics. Experimental works were carried out to investigate the local damage induced in the structure. Using the results from the experiment, they compare the results to the numerical study where good agreement was obtained with a relative error of 12.26%. Using validated numerical, they study the effect of damage region, size, and location. Following a similar step, Li et al., [20] studied the effect of damage presented in lattice sandwich structure to explore the behavior of the said structure under non-destructive evaluation (NDE). Experimental work has been done firstly for verification of simulation where the percentage error shown in the range of 5.06% to 12.77%. They also compared their experimental result to another reference in the study by Lou et al. [18] with a percentage error of -4.85% to 0.45%. Later, via the validated simulation, they lengthen their study to various topological designs of intact lattice sandwich structures. Besides, they also study the effect of damage with varied locations and damage extent of the lattice sandwich structure. Using validated, minimal experimental works were done.

Therefore, as an extension of the authors' previous work in [21] which experimentally explored the dynamic behavior and the effect of strut diameter design parameter of fused deposition modeling (FDM) lattice structure, this research aims to fill the gap and investigates the dynamic behavior of the lattice structure with the numerical result and compared to the experimentally attained result. In this research, through the finite element analysis (FEA) process, the influence of the strut diameter design parameter of additively manufactured (AM) body-centered cubic (BCC) lattice structures on its vibration characteristic for different types of AM materials is numerically studied.

METHODOLOGY

Finite element model of the lattice structure

The finite element method (FEM) was used to simulate the vibration and compressive behavior of the solid and lattice structure models. All the finite element (FE) models used in this study were designed using the universal designing software SolidWorks that were then imported into the ANSYS commercial FE software environment. A convergence test was conducted beforehand to govern the size of mesh elements that control the element sizes. This was done to ensure the reliability of the numerical results. The mesh convergence analysis was done by varying the size of the element that eventually increase the number of elements until the numerical result converged. The lattice structure models were made based on the BCC topological design with different strut diameter sizes as illustrated in Figure 1 (a). The lattice BCC one-unit cell was tessellated to form bar models with dimension of 160 mm x 30 mm x 15 mm each as shown in Figure 1 (b). The strut diameter size used ranges from 1.0 mm to 1.8 mm with 0.2 mm increment each. Hence, there were a total of six models including the solid bar model. Clamped-free (CF) boundary condition was considered for all the FE lattice and solid models to simulate cantilever beam behavior. The type of meshing element used was tetrahedrons. Both free vibration and static

deflection were performed by using modal analysis and structural analysis respectively. The material properties used are as tabulated in Table 1.

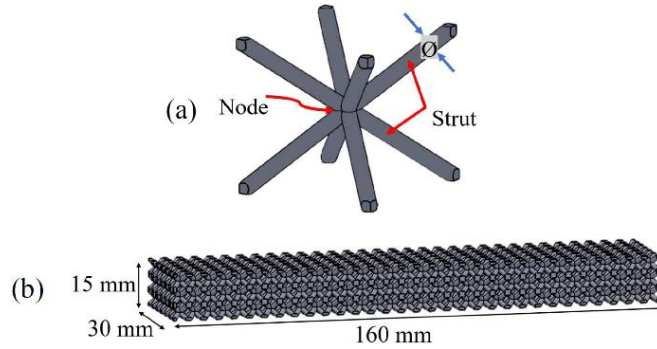


Figure 1. (a) One-unit cell of lattice BCC topological design; (b) tessellated lattice BCC topological design

Table 1. Material properties of FE models

Properties	Details		
Material	ABS	Titanium	Stainless steel
Density (kg/m ³)	1050	4430	8000
Young's Modulus (GPa)	3	114	193
Poison Ratio	0.35	0.33	0.28

Experiment

To corroborate the numerical results, actual experimental vibration testing was performed on the solid and lattice structure models with the same condition set in the simulation environment. For efficiency and purpose to reduce plastic waste which can pose a serious environmental threat [22]. Only two lattice models with strut diameters of 1.6 mm and 1.8 mm were fabricated using the FDM AM for experimental verification as experimentally validated numerical analysis with acceptable percentage error is imperative to ensure trueness of simulation of the feasibility of design and its suitability [23]. On the other hand, the solid sample was commercially sourced. The fabricated samples were excited with external impulsive point force at excitation location (yellow dot in Figure 2c) using an impact hammer with one clamped end as a boundary condition to mimic the single-end load-bearing application (known as clamped-free (CF) boundary condition) to a heavy test rig to serve as a rigid foundation.

The test rig used was made of heavy mild steel to suppress the system from any unwanted ambient vibrations. Figure 2 (a) and Figure 2 (b) show the schematic and actual experimental set-up respectively. The experimental set-up for vibration measurement consisted of an impact hammer to induce point force onto the lattice bar sample and an accelerometer sensor to measure the vibration amplitude. The input point force from the impact hammer and acceleration amplitude from the accelerometer were analyzed by the Dataphysics Quattro as a signal analyzer unit, the ratio of output acceleration and input force were measured from 1 Hz to 1200 Hz. The samples were excited at one-point force and the vibration response was measured at 5 different uniformly spaced measurement points as illustrated in Figure 2 (c). The experimental results are further discussed and compared with the numerical results acquired from the modal analysis from FE models.

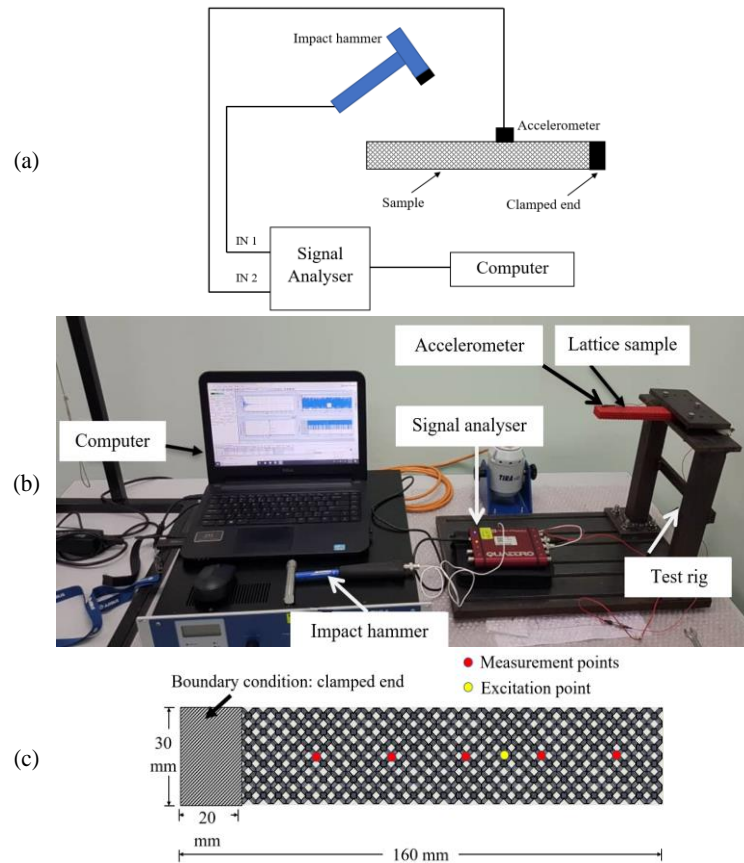


Figure 2. (a) Schematic diagram (b) actual experimental setup and (c) excitation and measurement points

RESULTS AND DISCUSSION

Mesh convergence analysis

Table 2 tabulates the results of the fundamental natural frequency for a one-layer lattice structure bar obtained from the convergence test. The initial size of the element chosen was 0.52 mm as assigned by the default generated meshing in ANSYS software. The results were plotted into a graph for better observation as shown in Figure 3. Based on Figure 3, the numerical result value of the fundamental natural frequency starts to become stable and converge at size element 0.49 mm up to 0.47 mm. Therefore, mesh element size no larger than 0.49 mm element size will be used for further numerical work as using smaller element size will result in a higher number of elements as shown in Figure 3 and eventually will cause longer simulation computational run time while producing similar output results. From the result, it can be seen that choosing the improper size of the element will result in deviated natural frequency values as the selected meshing element size did not fully represent the model during simulation. Hence, it is important to conduct a mesh convergence test for accurate numerical results.

Table 2. Result of convergence analysis for the FE models for the lattice structure

Element size (mm)	Number of elements	First mode natural frequency (Hz)
0.52	509143	22.42
0.51	634578	22.41
0.50	637459	22.40
0.49	641116	22.39
0.48	648469	22.39
0.47	650165	22.39

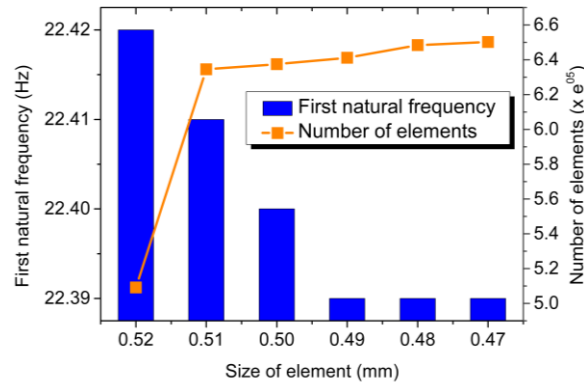


Figure 3. The trend of convergence test for lattice structure

Experimental result

Figure 4 shows the frequency response function (FRF) graphs obtained through experimental work on two samples of ABS lattice structures as well as the solid ABS sample. The test was done multiple times for each sample to ensure the consistency of the produced results. The fundamental natural frequency values were extracted and tabulated in Table 3. From the results shown, it can be seen that for both numerical and experimental, lattice structures with the smallest strut diameter exhibited lower natural frequency values and solid bar exhibited almost twice the natural frequency value. An increase in strut diameter will increase the total area moment of inertia due to an increased cross-sectional area which directly influences the stiffness of the lattice structure bar [19]. The relationship between the natural frequency to stiffness and area moment of inertia is as in equation (1) where CF boundary condition bars were assumed to behave as cantilever beam during the experiment.

$$\omega_n = \sqrt{\frac{k}{m}} = \sqrt{\frac{3EI}{ml^3}} \quad (1)$$

where ω_n is the natural frequency [Hz], k is the stiffness [N/m] m is the mass [kg] l is the length of the lattice structure bar [m] I is the total area moment of inertia and E is the elastic modulus of ABS material. The comparison between the numerical and experimental results for both solid and lattice structure ABS models shows good agreement. The percentage error, with respect to the experimental results, between the two values, is shown in the fourth column. As a result, for all models with the largest error seen by the lattice structure with a 1.6 mm strut diameter, the percentage error is less than 10.87%, whereas the lowest percentage error is 3.58% seen by the solid ABS model. Moreover, the natural frequencies obtained through numerical work are slightly higher than that of experimental work. This is because the ideal clamped boundary condition in the experimental setup cannot be achieved as opposed to the absolute clamped boundary condition set in the FE models [24]. Besides that, the manufacturing process can also affect the results in experimental work as the fabricated lattices suffer from manufacturing defects that typically have a slight geometrical deviation from modeled lattices [18-19]. Besides that, it is known that the FDM models prone to have air gaps and voids within the produced samples [25]. These effects are not considered in the relatively ideal FE models. In addition, this is also shown by the solid ABS with the least error due to minimal manufacturing defects as opposed to the additively manufactured lattice structure bar.

Table 3. Comparison of natural frequency for the finite element analysis and experimental for the 1st mode of vibration only

Design of FE models	First mode of natural frequency (Hz)		Error (%)
	Numerical	Experimental	
1.6 mm	75.40	68.00	10.87
1.8 mm	87.67	82.00	6.91
Solid ABS	153.31	159.00	3.58

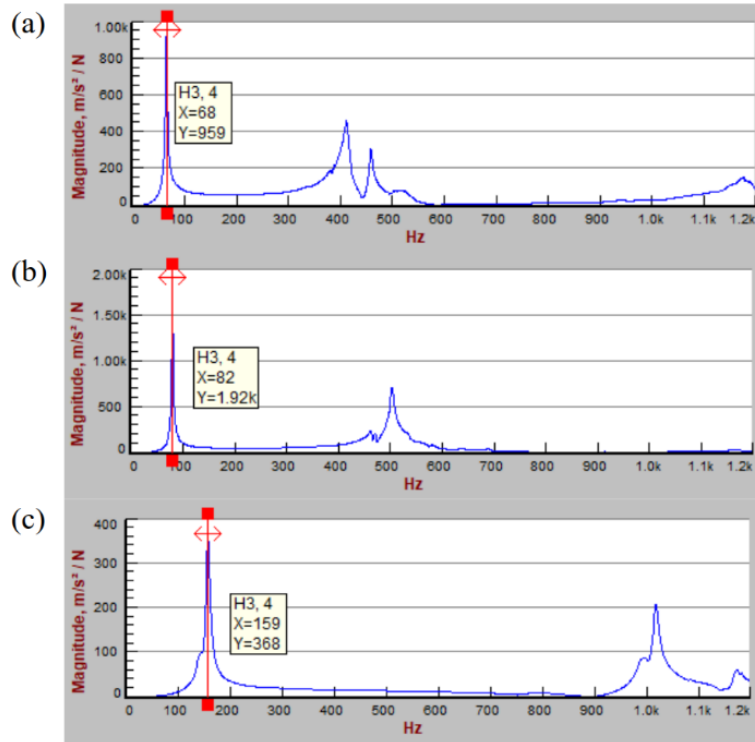


Figure 4. FRF graphs from experimental work for (a) 1.6 mm (b) 1.8 mm and (c) solid ABS

Therefore, it is clear that the FE models developed will reliably predict the natural frequencies of samples of lattice and solid bars. A variety of numerical studies were carried out using the experimentally validated FE models to further investigate and observe the patterns as well as to use various material assignments namely stainless steel and titanium which is otherwise costly and time consuming to manufacture to be tested in real experimental work [26]. These materials are commonly used in metal additive manufacturing techniques [15].

Modal analysis

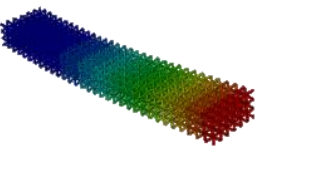
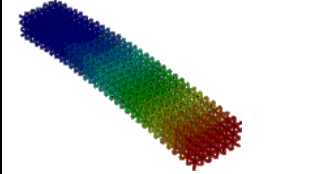
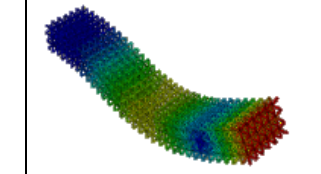
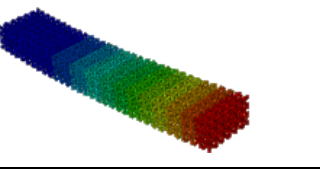
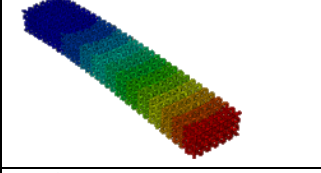
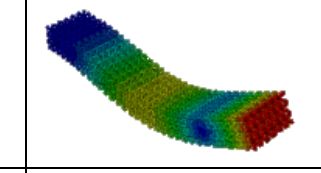
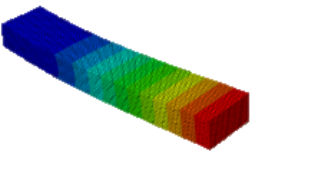
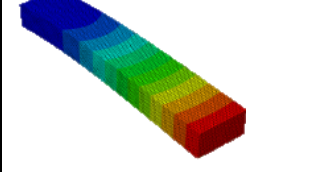
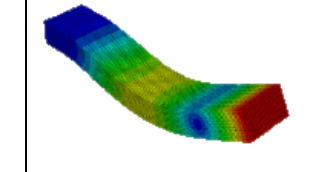
Table 4 tabulates the first three natural frequency values of the ABS material derived from the modal analysis and shown in Figure 5. Based on Figure 5, it can be seen that the solid bar model exhibited much higher frequency values as compared to the lattice bar models. Meanwhile, amongst lattice models, the largest strut diameter 1.8 mm sample provided the highest natural frequency values as predicted for all three modes because of increased lattice stiffness [19,21]. Hence, an increase in the strut diameter will result in higher natural frequency values. From Table 4, the numerical result for the first vibration mode shows an increment of average around 12 Hz in natural frequency as the strut diameter increase by 0.2 mm each. Meanwhile, for the second and third modes of vibrations, the natural frequency increased at averagely around 20 Hz and 70 Hz respectively.

Table 4. Modal analysis for 1st, 2nd, and 3rd modes of vibration of ABS material

Numerical Results			
Model	Natural frequency (Hz)		
	First mode	Second mode	Third mode
ABS			
1.0 mm	41.31	79.38	256.62
1.2 mm	52.13	99.34	321.70
1.4 mm	63.54	120.13	389.60
1.6 mm	75.40	140.02	459.81
1.8 mm	87.67	160.65	533.38
Solid	153.31	247.78	963.60

Table 5 shows the first three vibration mode shapes of ABS solid as well as lattice bar models. From Table 5, it can be seen that the mode shapes displayed are similar to each other which demonstrates the typical mode shapes of CF boundary condition [27]. For the first three modes of vibration, the dark blue region in these figures from Table 5 indicates the nodal displacements, showing the area where the displacement is close to zero. The red area shows the high amplitude of the first three vibration modes, where the highest displacement occurred. The first three natural frequency values of the stainless steel and titanium materials obtained from the modal analysis are tabulated in Table 6 and the trend is illustrated in Figure 6 and Figure 7 respectively.

Table 5. The first three mode shapes of lattice structure and solid design

Model	Mode shapes of solid and lattice structure design		
	First mode	Second mode	Third mode
1.0			
1.6			
Solid			

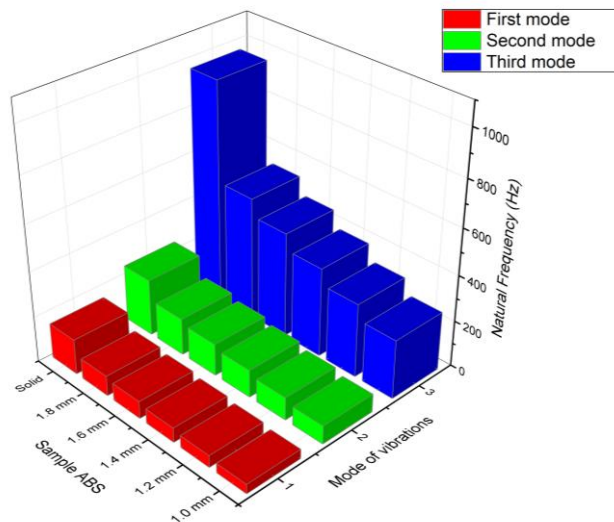


Figure 2. The natural frequency values of solid and lattice structures of ABS material

As expected, a similar trend can be observed for stainless steel and titanium materials where the solid model exhibited much higher frequency values as compared to the lattice models and lattice models with the largest strut diameter 1.8 mm produced the highest natural frequency values as compared to other strut diameter lattices. However, for both stainless steel and titanium, with an increment of 0.2 mm in strut diameter each, roughly around 35 Hz, 60 Hz, and 200 Hz of increased natural frequency values as opposed to ABS material at 12 Hz, 20 Hz, and

70 Hz for the first, second and third mode of vibrations can be observed respectively. It should be noted that the titanium material has substantially higher natural frequency values at around an average of 4%.

Table 6. Modal analysis for 1st, 2nd, and 3rd vibration modes of stainless steel and titanium materials

Numerical Results			
Model	Natural frequency (Hz)		
	First mode	Second mode	Third mode
Stainless steel			
1.0 mm	118.62	227.88	737.05
1.2 mm	149.57	284.99	932.46
1.4 mm	182.21	344.54	1117.80
1.6 mm	216.42	402.32	1320.60
1.8 mm	252.14	462.32	1533.20
Solid	589.22	1106.50	3531.70
Titanium			
1.0 mm	123.55	237.42	767.61
1.2 mm	155.88	297.05	962.12
1.4 mm	189.98	359.18	1165.00
1.6 mm	225.48	418.87	1375.30
1.8 mm	262.52	480.78	1595.70
Solid	610.09	1144.10	3652.80

This is because the main features of titanium as compared to stainless steel is around 60% lower density which would result in lower mass. Mines [28] stated that replacing stainless steel with titanium for the body-centered cubic case increases specific stiffness by a factor of 33%. A combination of both higher stiffness and lower mass would result in higher natural frequency values as evidently shown by the simulation results.

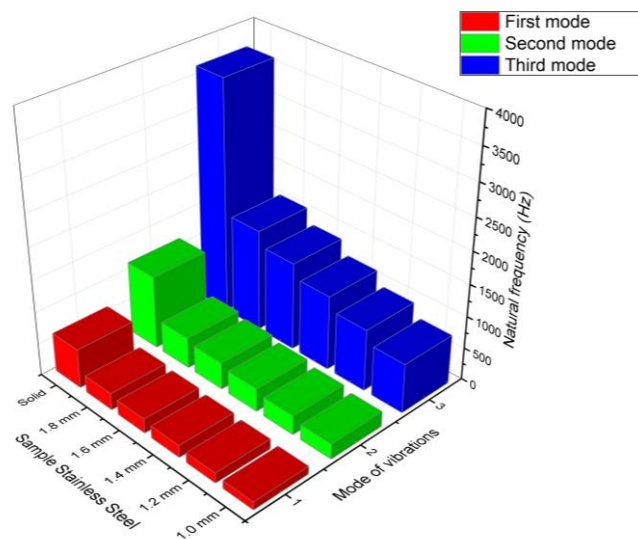


Figure 6. The natural frequency values of solid and lattice structures of stainless steel material

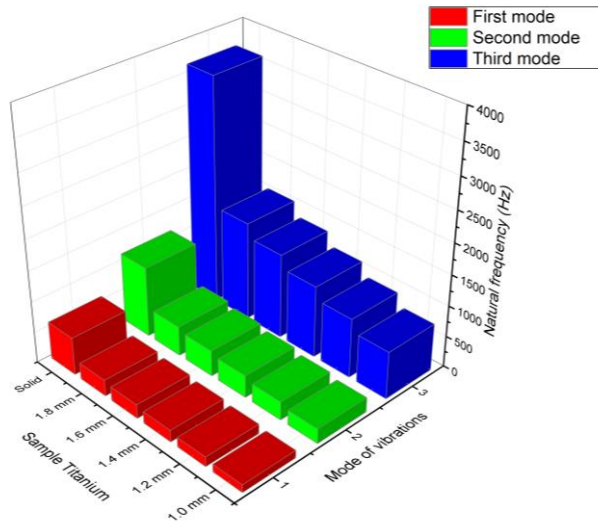


Figure 3. The natural frequency values of solid and lattice structures of titanium material

Static load-deflection analysis

To support the modal analysis result in the previous section, static structural analysis using ANSYS was also computed to determine the stiffness of each model. The maximum force applied and the maximum deflection recorded and tabulated in Table 7. Meanwhile, Figure 8 shows the linear graph of force against the displacement of the ABS lattice and solid models where the stiffness is defined by the ratio of compression force to the displacement of the plot since the stiffness-displacement relationship is still linear for a small force [19].

Table 7. Maximum force, maximum deflection, and stiffness of ABS material models

Model	Max. Force, F (N)	Max. Deflection, x ($\times 10^{-4}$ m)	Stiffness, k (kN/m)
Solid ABS	10.0	3.152	31.73
1.8 mm	10.0	29.41	3.40
1.6 mm	10.0	49.44	2.02
1.4 mm	10.0	90.11	1.11
1.2 mm	10.0	197.8	0.51
1.0 mm	10.0	438.3	0.23

As expected, the lattice structure with the lowest strut diameter showed the biggest deflection under a similar force. The solid ABS model showed the highest stiffness with 31.73 kN/m. Meanwhile, for lattice structure models, the stiffness values decrease consecutively as the strut diameter decreases from 1.8 mm to 1.0 mm at 31.73 kN/m, 3.40 kN/m, 2.02 kN/m, 1.11 kN/m, 0.51 kN/m, 0.23 kN/m respectively. The solid ABS model has higher stiffness in contrast to the ABS lattice structure bar as it has a bigger cross-sectional area which affects the total area moment inertia as opposed to lattice structure models [19]. The stiffness of the lattice is proportionate to its total area moment of inertia. Consequently, a rise in the total area moment of inertia increases the stiffness and consequently leads to higher natural frequency values as manifestly shown in the experimental and numerical results above.

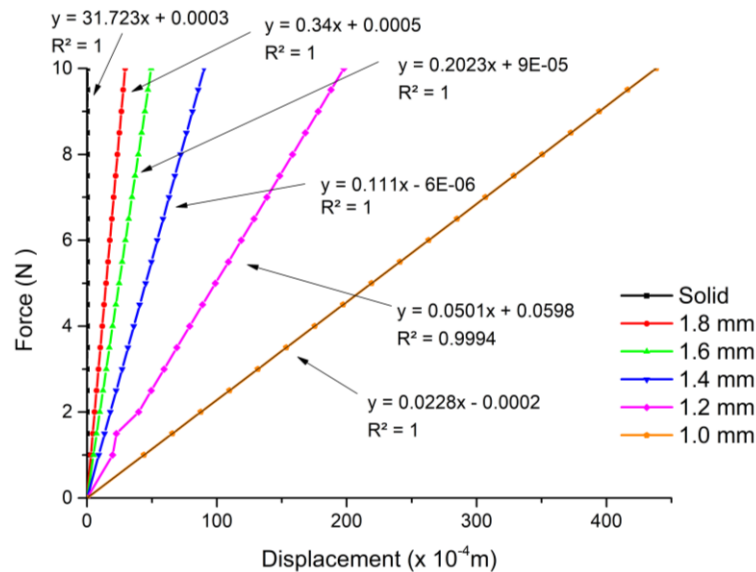


Figure 4. Force- displacement plot for ABS material models

CONCLUSION

The effect of the size of the strut diameter on the natural frequencies of the lattice structure is studied through experimental vibration testing and finite element method (FEM) in the present paper. The main findings can be summarized as follow, the natural frequency values increase as the size of strut diameter increase where natural frequencies obtained from the FE method and experimental method show good agreement with an acceptable maximum of 11% percentage error values. Numerical result for the first, second and third vibration modes for the ABS material show an increment of average around 12 Hz, 20 Hz and 70 Hz in natural frequency respectively as the strut diameter increase by 0.2 mm each. Meanwhile, stainless steel and titanium show 35 Hz, 60 Hz, and 200 Hz increase in natural frequency for the first three vibration modes. Therefore, the experimentally validated FE models developed can be used for exploration on many other materials as conducted in the present paper for stainless steel and titanium. FE model developed can be used as well for other design parameters, lattice topological designs, existence of damage within the structure without having to conduct experimental work which in the end will reduce cost and material consumptions for sustainability.

ACKNOWLEDGEMENT

The authors acknowledge the financial support from Zamalah Scheme, Universiti Teknikal Malaysia Melaka

REFERENCES

- [1] M.F. Abdollah and R. Hassan, "Preliminary Design of Side Door Impact Beam for Passenger Cars using Aluminium Alloy," *Journal of Mechanical Engineering and Technology*, Vol. 5, (1), Pp. 11–18, 2013. [Online]. Available: <http://eprints2.utm.edu.my/10058/1/jmet.vol5.no1.fullpaper2.pdf>.
- [2] R. Budynas and K. Nisbett, "Shigley's Mechanical Engineering Design, Ninth Edition," McGraw Hill Inc., 2009.
- [3] E.R.H. Fuchs, F.R. Field, R. Roth, and R.E. Kirchain, "Strategic materials selection in the automobile body: Economic opportunities for polymer composite design," *Composites Science and Technology*, 2008. doi: 10.1016/j.compscitech.2008.01.015.
- [4] K. Markus, "Size optimization of aircraft structures," KTH Royal Institute of Technology, 2008.
- [5] M. Pournazeri, A. Khajepour, and Y. Huang, "Improving energy efficiency and robustness of a novel variable valve actuation system for engines," *Mechatronics*, 2018. doi: 10.1016/j.mechatronics.2018.02.002.
- [6] A. Solouk, M. Shakiba-Herfeh, J. Arora, and M. Shahbakhti, "Fuel consumption assessment of an electrified powertrain with a multi-mode high-efficiency engine in various levels of hybridization," *Energy Conversion*

- and Management, 2018. doi: 10.1016/j.enconman.2017.10.073.
- [7] M.A. Badie, E. Mahdi, and A.M.S. Hamouda, “An investigation into hybrid carbon/glass fiber reinforced epoxy composite automotive drive shaft,” *Materials and Design*, Vol. 32, (3), Pp. 1485–1500, 2011. doi: 10.1016/j.matdes.2010.08.042.
- [8] D.H. Kim, D.H. Choi, and H.S. Kim, “Design optimization of a carbon fiber reinforced composite automotive lower arm,” *Composites Part B: Engineering*, Vol. 58, Pp. 400–407, 2014. doi: 10.1016/j.compositesb.2013.10.067.
- [9] J. W. McAuley, “Global Sustainability and Key Needs in Future Automotive Design,” *Environmental Science and Technology*, 2003. doi: 10.1021/es030521x.
- [10] Z. Ozdemir et al., “Energy absorption in lattice structures in dynamics: Experiments,” *International Journal of Impact Engineering*, 2016. doi: 10.1016/j.ijimpeng.2015.10.007.
- [11] I. Maskery et al., “An investigation into reinforced and functionally graded lattice structures,” *Journal of Cellular Plastics*, 2017. doi: 10.1177/0021955X16639035.
- [12] R. Hasan, “Progressive collapse of titanium alloy micro-lattice structures manufactured using selective laser melting,” University of Liverpool, 2013.
- [13] G. Cricri, M. Perrella, and C. Calì, “Honeycomb failure processes under in-plane loading,” *Composites Part B: Engineering*, 2013. doi: 10.1016/j.compositesb.2012.07.032.
- [14] M. Ashby, et al., “Metal Foams: A Design Guide,” *Applied Mechanics Reviews*, 2001. doi: 10.1115/1.1421119.
- [15] T.D. Ngo, A. Kashani, G. Imbalzano, K.T.Q. Nguyen, and D. Hui, “Additive manufacturing (3D printing): A review of materials, methods, applications and challenges,” *Composites Part B: Engineering*, Vol. 143. Elsevier Ltd, Pp. 172–196, 2018. doi: 10.1016/j.compositesb.2018.02.012.
- [16] N. Weake, M. Pant, A. Sheoran, A. Haleem, and H. Kumar, “Optimising parameters of fused filament fabrication process to achieve optimum tensile strength using artificial neural network,” *Evergreen*, Vol. 7, (3), Pp. 373–381, 2020. doi: 10.5109/4068614.
- [17] R.A.W. Mines, “On the characterisation of foam and micro-lattice materials used in sandwich construction,” 2008. doi: 10.1111/j.1475-1305.2008.00399.x.
- [18] J. Lou, L. Wu, L. Ma, J. Xiong, and B. Wang, “Effects of local damage on vibration characteristics of composite pyramidal truss core sandwich structure,” *Composites Part B: Engineering*, 2014. doi: 10.1016/j.compositesb.2014.02.012.
- [19] W.P. Syam, W. Jianwei, B. Zhao, I. Maskery, W. Elmadih, and R. Leach, “Design and analysis of strut-based lattice structures for vibration isolation,” *Precision Engineering*, 2018. doi: 10.1016/j.precisioneng.2017.09.010.
- [20] J. Lou, L. Wu, L. Ma, J. Xiong, and B. Wang, “Effects of local damage on vibration characteristics of composite pyramidal truss core sandwich structure,” *Composites Part B: Engineering*, 2014. doi: 10.1016/j.compositesb.2014.02.012.
- [21] M.S. Azmi, R. Hasan, R. Ismail, N.A. Rosli, and M.R. Alkahari, “Static and dynamic analysis of FDM printed lattice structures for sustainable lightweight material application,” *Progress in Industrial Ecology*, 2018. doi: 10.1504/PIE.2018.097063.
- [22] P.P.D.K. Wulan, J.A. Ningtyas, and M. Hasanah, “The effect of nickel coating on stainless steel 316 on growth of carbon nanotube from polypropylene waste,” *Evergreen*, 2019. doi: 10.5109/2328411.
- [23] M. Sharma and M. Soni, “A musculoskeletal finite element study of a unique and customised jaw joint prosthesis for the Asian populace,” *Evergreen*, 2020. doi: 10.5109/4068615.
- [24] B. Li, Z. Li, J. Zhou, L. Ye, and E. Li, “Damage localization in composite lattice truss core sandwich

- structures based on vibration characteristics,” *Composite Structures*, 2015. doi: 10.1016/j.compstruct.2015.02.046.
- [25] N.K. Maurya, V. Rastogi, and P. Singh, “Experimental and computational investigation on mechanical properties of reinforced additive manufactured component,” *Evergreen*, 2019. doi: 10.5109/2349296.
- [26] S.L.S. Chauhan and S.C. Bhaduri, “Structural analysis of a four-bar linkage mechanism of prosthetic knee joint using finite element method,” *Evergreen*, 2020. doi: 10.5109/4055220.
- [27] A. Sahin and A. Bayraktar, “MATLAB for All Steps of Dynamic Vibration Test of Structures,” in *Applications from Engineering with MATLAB Concepts*, 2016.
- [28] R. Mines, “Parent Materials and Lattice Characterisation for Metallic Microlattice Structures,” in *SpringerBriefs in Applied Sciences and Technology*, 2019.